iScience

CellPress
OPEN ACCESS

Article

Caenorhabditis elegans neuropeptide NLP-27 enhances neurodegeneration and paralysis in an opioid-like manner during fungal infection

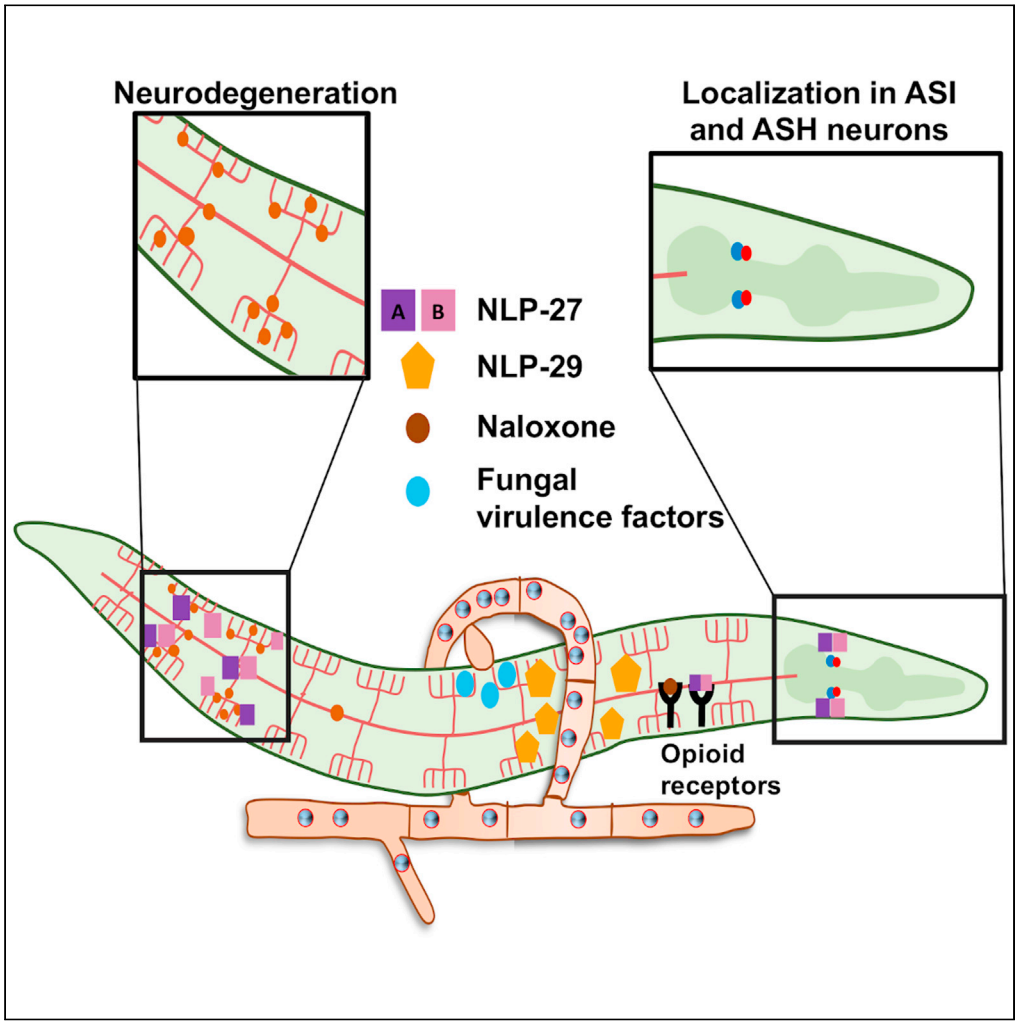

Maria Pop, Anna-Lena Klemke, Lena Seidler, ..., Vanessa Baust, Elke Wohlmann, Reinhard Fischer

reinhard.fischer@KIT.edu

Highlights

Induction of neuropeptides during fungal infection

Induction of paralysis during fungal infection

NLP-27 enhances neurodegeneration

NLP-27 contains the YGGYG opioid motif and may be processed

Pop et al., iScience 27, 109484
April 19, 2024
https://doi.org/10.1016/j.isci.2024.109484

iScience

CellPress
OPEN ACCESS

Article

Caenorhabditis elegans neuropeptide NLP-27 enhances neurodegeneration and paralysis in an opioid-like manner during fungal infection

Maria Pop,[1] Anna-Lena Klemke,[1] Lena Seidler,[1] Nicole Wernet,[1] Pietrina Loredana Steudel,[1] Vanessa Baust,[1] Elke Wohlmann,[1] and Reinhard Fischer[1,2,*]

SUMMARY

The nervous system of metazoans is involved in host-pathogen interactions to control immune activation. In *Caenorhabditis elegans*, this includes sleep induction, mediated by neuropeptide-like proteins (NLPs), which increases the chance of survival after wounding. Here we analyzed the role of NLP-27 in the infection of *C. elegans* with the nematode-trapping fungus *Arthrobotrys flagrans*. Early responses of *C. elegans* were the upregulation of *nlp-27*, the induction of paralysis (sleep), and neurodegeneration of the mechanosensing PVD (Posterior Ventral Process D) neurons. Deletion of *nlp-27* reduced neurodegeneration during fungal attack. Induction of *nlp-27* was independent of the MAP kinase PMK-1, and expression of *nlp-27* in the hypodermis was sufficient to induce paralysis, although NLP-27 was also upregulated in head neurons. NLP-27 contains the pentapeptide YGGYG sequence known to bind the human μ- and κ-type opioid receptors suggesting NLP-27 or peptides thereof act on opioid receptors. The opioid receptor antagonist naloxone shortened the paralysis time like overexpression of NLP-27.

INTRODUCTION

The nervous and the immune system both play a role in host-pathogen interactions to ensure appropriate and specific immune responses against pathogens.[1] However, the underlying complex mechanisms of neural regulation are not yet well understood. Neuropeptides are chemical messengers with roles in synaptic signaling as well as in the innate immune response and age-related neurodegeneration.[2,3] Genome analyses suggest the presence of at least 48 neuropeptides in *C. elegans*. One class of neuropeptides is *neuropeptide-like proteins* (NLPs), diverse peptides grouped into 11 categories based on certain repeating amino acid motifs.[3]

In *C. elegans* NLPs may be expressed and released by neurons, but some are also expressed in non-neuronal tissues such as the hypodermis.[4] Neuropeptides and NLPs are encoded as precursor molecules and are post-translationally processed into bioactive peptides that typically bind to GPCRs to modulate many physiological functions.[3,4] Other NLPs act as antimicrobial peptides (AMPs).[5] Some AMPs are highly expressed in mouse microglia cells suggesting roles beyond the antimicrobial activities.[6] Also, some neuropeptides control the unfolded protein response in the ER of glia cells.[7] Taken together, neuropeptides and NLPs appear to be more versatile as the name implies and serve different functions, many of which are currently unknown.

Some NLP-encoding genes are clustered in the *C. elegans* genome, and the *nlp-29* cluster is one of the best studied. It consists of NLP-27, 28, 29, 30, 31, and 34. They are all characterized by YGGYG amino acid repeats in their sequences.[5,8,9] NLP-31 is part of the innate immune response to infection with the predatory fungus *Drechmeria coniospora* and has antifungal activity *in vitro* against *Aspergillus fumigatus* and other fungi.[5] The closely related, epidermally expressed NLP-29 is an antimicrobial peptide that causes aging-associated dendrite neurodegeneration in PVD neurons dependent on TIR-1 (toll-interleukin 1 repeat protein) and the MAP kinase PMK-1.[8] PVD neurons are mechanosensory neurons with highly ordered dendritic branches that respond to high threshold mechanical stimuli.[10] *nlp-29* expression increases with age and artificial overexpression causes early onset of dendrite degeneration.[5,8] In comparison, NLP-31 does not play a role in neurodegeneration, despite the high sequence conservation with NLP-29.[8] NLP-29 together with another dozen neuropeptides, including NLP-27, promotes sleep after epidermal wounding in a RIS-dependent manner which increases the survival chances of the nematode.[11] Interestingly, *nlp-27* is downregulated in bacterial infections with *P. aeruginosa*, *S. marcescens*, *Enterococcus faecalis*, *Bacillus thuringiensis*, and *Photorhabdus luminescens* and upregulated in fungal infections with *D. coniospora* or *Harposporium* spp..[12,13] NLP-27 is expressed in the hypodermis, the first line of defense, suggesting antimicrobial activity like NLP-31.[5] However, NLP-27 is also expressed in ASI neurons, and unlike the other peptides of the cluster, NLP-27 is not upregulated by osmotic stress.[14] Hence, the *nlp-29* gene cluster encodes six related NLPs with specific and overlapping functions and responding to different endo- and exogenous cues.

[1]Karlsruhe Institute of Technology (KIT) - South Campus, Institute for Applied Biosciences, Department of Microbiology, Fritz-Haber-Weg 4, 76131 Karlsruhe, Germany
[2]Lead contact
*Correspondence: reinhard.fischer@KIT.edu
https://doi.org/10.1016/j.isci.2024.109484

An important family of nematode pathogens in natural habitats are predatory nematode-trapping fungi (NTF) like *Arthrobotrys flagrans* (formerly *Duddingtonia flagrans*).[15] The NTF *A. flagrans* develops a trapping network consisting of several adhesive rings in which nematodes like *C. elegans* can be trapped. Sophisticated interkingdom communication regulates trap formation in the presence of sufficient numbers of nematodes.[16–19] Trap formation requires cues about the presence of nematodes in the surrounding as well as complex cell-to-cell communication for ring formation and closure.[19–21] After the nematode is immobilized in the trap, the fungus pierces the nematode cuticle with a penetration peg and subsequently develops mycelium inside the nematode body. The nematode immune response is probably triggered by the cuticular damage as well as by small secreted proteins (SSP).[16,22] CyrA (cysteine-rich protein A), the first characterized SSP, is secreted by *A. flagrans* and shortens the lifespan of the nematode when expressed heterologously in the nematode. Another fungal SSP is PefD (putative effector D), which localizes in nuclei of *C. elegans* when expressed in the nematode.[22,23] Whether *C. elegans* NLPs (AMPs) are targets for such SSPs remains to be determined.

Here we show that NLP-27 plays a role in infection-induced paralysis of *C. elegans* during *A. flagrans* attack. NLP-27 induction is *pmk-1* independent and induces dendrite neurodegeneration in PVD neurons. NLP-27 is predicted to contain a neuropeptide cleavage site, and indeed one of the cleaved peptides was sufficient to cause neurodegeneration. *A. flagrans* infection caused PVD dendrite neurodegeneration starting from the trapping site.

Understanding how the nervous system is connected and overlaps with the innate immune response during infection holds great therapeutic potential as well as understanding fungal-induced acute neurodegeneration during infection.

RESULTS

The neuropeptide-like protein NLP-27 is upregulated in ASI and ASH neurons during *A. flagrans* fungal infection

The hypodermally expressed *nlp-29* cluster was shown to play an important role in microbial infections.[5,8] Therefore, we tested whether the cluster may play a role during the attack of the predatory fungus *A. flagrans*. Whereas bacteria infect *C. elegans* mainly through the intestine, *A. flagrans* captures *C. elegans* with adhesive trapping structures and penetrates the cuticle from outside. This can happen at any place along the *C. elegans* body. Since after cuticle penetration, the hypodermis is the first tissue *A. flagrans* encounters, it is likely that the attack stimulates an immune response in the hypodermis. To test this, the expression of *nlp-29*-cluster genes (*nlp-27*, *nlp-28*, *nlp-29*, *nlp-31*, and *nlp-34*) (Figure 1A) after infection was monitored by qRT-PCR (Figures 1A and 1B). Young adult nematodes were infected with *A. flagrans*. Briefly, low nutrient agar (LNA) infection plates were prepared by co-incubating *A. flagrans* spores with nematodes for 24 h at 28°C for trap induction. Then nematodes were washed off the plate with sterile water and synchronized young adults were added on the induced fungal mycelium and incubated for 4 h. After this incubation time, nematodes were collected, and total RNA was extracted and used for the qRT-PCR experiments. All *nlp-29* cluster genes were upregulated to different extents after infection with *A. flagrans* (Figure 1B).

Given the anti-microbial activity of some NLPs encoded in the *nlp-29* cluster, it was possible that *C. elegans* reacts to the *A. flagrans* attack with a local response at the trap site instead of a systemic response throughout the body. To distinguish between local or general upregulation of the *nlp-29*-cluster genes, we used a transcriptional reporter strategy based on GFP or wrmScarlet as fluorescent proteins. We fused the promoters of *nlp-27*, *nlp-29*, and *nlp-31* to the corresponding coding regions of the fluorescent proteins (Figures 1C–1F). In addition, we added a nuclear localization signal. Promoter activity can thus be unambiguously resolved by fluorescent nuclei and easily distinguished from background fluorescence of the cells. The plasmids were injected into the *unc-119* mutant strain to rescue the motility phenotype in positive transformants, and they were expressed as extrachromosomal arrays. The localization of GFP or wrmScarlet was performed by adding synchronized young adults onto LNA containing 15 mM NaN_3. The *nlp-29* and *nlp-31* promoters appeared to be active mostly in the intestine and hypodermis in the absence of *A. flagrans* (control) (Figure 1C). To visualize the signals during infection, microscopy slides were prepared by co-incubating spores and nematodes on LNA for 24 h to induce trap formation. Then nematodes were washed off, and fresh young synchronized transgenic adult nematodes were added to the fungus. The expression of GFP under *nlp-29* promoter control showed a stronger signal at the trap site, while the wrmScarlet signal under *nlp-31* promoter control showed a general response to infection and was upregulated throughout the nematode body (Figure 1D). *nlp-31* appears to be expressed in the head area under normal conditions, but during infection, the signal was mostly increased in the body area, while *nlp-29* does not seem to have any neuronal localization during infection or under normal conditions but shows a trap localization (Figures 1C and 1D). To further support our assertion that *nlp-27* is not upregulated at the trapping site and find out whether there is background expression in the gut or genuine signal from GFP/wrmScarlet, the fluorescence seen in Figures 1C–1F was quantified in Figure S1. In comparison, the *nlp-27* promoter fusion showed an increased signal intensity in the nuclei of the hypodermis with the exception at the trap site (Figures 1F and S2).

Interestingly, *nlp-27* was upregulated in the head area during infection, and this upregulation appeared to be independent of the place of the trap (Figures 2A–2C). This result suggested a distinct role of *nlp-27* neuronal expression during infection. To test if *nlp-27* induction was already caused by the first step of *A. flagrans* infection, namely wounding of the cuticle and hypodermis, we sterile wounded young adults with a microinjection needle. The same pattern of *nlp-27* promoter activity was observed during the infection with a strong expression in the head region (Figure 2D).

nlp-27 expression was documented in one neuron pair, the ASI.[3] However, our promoter-reporter line expressing *nlp-27(p)::NLS-wrmScarlet* showed additional signals in other un-identified neurons (Figure S3A). To determine the identity of the other pair of neurons, we co-expressed *dcar-1(p)::NLS-GFP* along with *nlp-27(p)::NLS-wrmScarlet*. DCAR-1 is a GPCR known to be expressed in the ASI and ASH neurons among other tissues.[24] It is also activated by dihydrocaffeic acid which leads to *nlp-29* gene cluster upregulation.[25] Fluorescent signals were co-localizing in the ASH and ASI neurons (Figure 2E). A marker strain with labeling specifically only ASI and ASH neurons is not available.

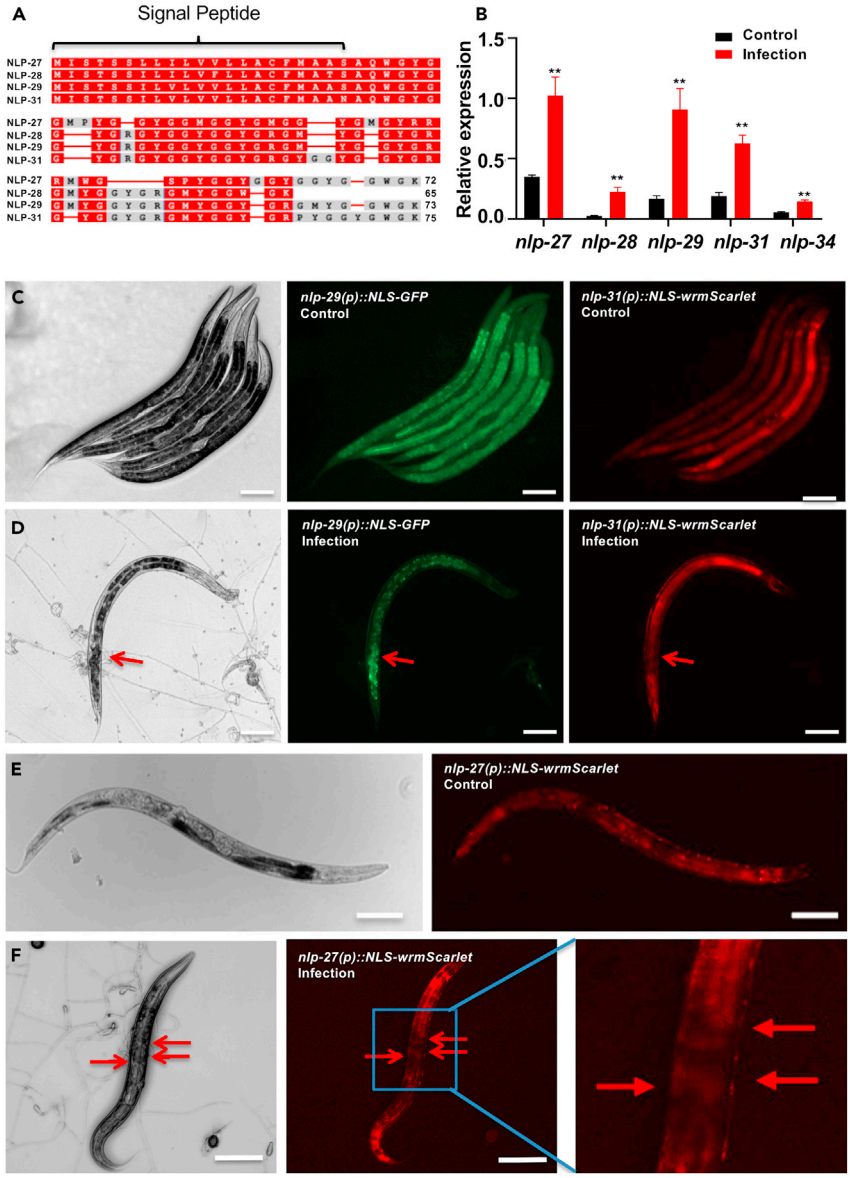

Figure 1. Analysis of the expression changes of the *nlp-29* gene cluster in *C. elegans* after infection with *A. flagrans*

(A) Alignment of the peptides encoded by the *nlp-29* gene cluster without NLP-34.

(B) Relative expression of the *nlp-29* gene cluster genes during infection with *A. flagrans* determined by qRT PCR with actin for normalization. Young adult nematodes were co-incubated with *A. flagrans* for 24 h and total RNA was extracted using the TRIzol method, **p < 0.01. (C–F) Expression analyses using promoter-reporter assays with fluorescence microscopy. Promoters of *nlp-29*, *nlp-31*, and *nlp-27* were fused to a DNA fragment encoding an NLS and to the wrmScarlet or GFP-coding gene.

(C) Expression of *nlp-29* and *nlp-31 in nlp-29(rfl5)* in uninfected control nematodes and (D) during infection with *A. flagrans*.

(E) Expression of *nlp-27* in *nlp-27(rfl2)* in uninfected control nematodes and (F) during infection with *A. flagrans*. The fluorescence signals of Figures 1C–1F were quantified (Figure S1). The arrows indicate the site of infection. The scale bar represents 100 μm.

Therefore, *nlp-27* expression was also studied by DiO staining. DiO stains the amphid neurons (Figure S3B).[26] The results do not exclude that NLP-27 is also expressed in some other neurons, but it indicates a complex chemosensory regulation in neurons. The *nlp-29* cluster, of which *nlp-27* is part of, has long been proposed to have antimicrobial activity.[5] However, the AMP function has been inferred to the whole cluster based on NLP-31 antimicrobial activity. A neuronal expression of *nlp-27* might be indicative of a distinct function for this neuropeptide, other than antimicrobial.

ASIs are polymodal sensory neurons involved in the modulation of worm behaviors such as *dauer* formation,[27] suppression of sexual attraction behavior,[28] negative modulation of thermotaxis,[29] avoidance of the smell of pathogenic bacteria after ingestion,[30] and acute CO_2

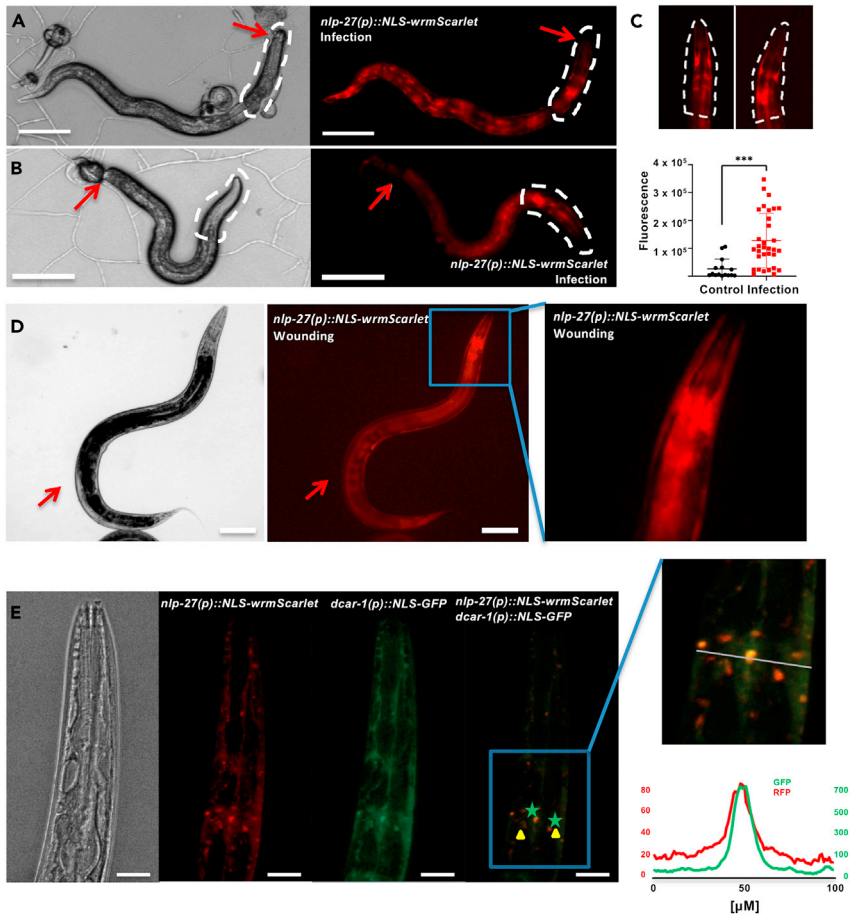

Figure 2. *nlp-27* is induced in the head area of *C. elegans* after infection with *A. flagrans* and after wounding

Induction of *nlp-27* in *nlp-27(rfl2)* after trapping of the nematode in the (A) head and (B) tail area. The arrows indicate the site of infection. The scale bar represents 100 µm.

(C) Comparison of the fluorescence of the reporter construct in untrapped and in trapped nematodes. The above panels show the marked area of the pharynx, while the graph shows the total cell fluorescence measured in ImageJ. Unpaired Student's t test was calculated for all experiments. Ns $p > 0.05$, *$p < 0.05$, **$p < 0.01$, ***$p < 0.001$.

(D) Visualization of the fluorescence of the reporter construct after wounding in *nlp-27(rfl8)*. The scale bar represents 100 µm.

(E) Expression of *nlp-27* in ASI and ASH head neurons *nlp-27(rfl2)*. Yellow triangle and green star point at ASI and ASH neurons. The graph represents the GFP, and wrmScarlet (RFP) intensity measured with ImageJ along the line shown in the close-up. The scale bar represents 20 µm.

avoidance.[31] During infection, ASI neurons are involved in pathogen avoidance while ASH downregulate the immune response.[32] Moreover, both pairs of neurons express *dcar-1*, the GPCR upstream of *nlp-27* regulatory pathway. DCAR-1 has been shown to be involved in the upregulation of *nlp-27* expression when the nematode is exposed to dihydrocaffeic acid (DHCA) and the endogenous ligand for DCAR-1 is HPLA (4-hydroxyphenyllactic acid) a tyrosine derivative shown to be increased in patients with sepsis.[25,33] The nematode also shows avoidance phenotype when exposed to DHCA, and expressing *dcar-1* only in ASI, ASH, and PVQ neurons is enough to restore the avoidance phenotype. Therefore, there is evidence for a complex interplay between the ASI and ASH, ASI and pathogen and DHCA avoidance and perhaps the endogenous activation of the *dcar-1* which leads to *nlp-27* expression. Focusing on these two pairs of neurons improves our knowledge on how ASI and ASH might modulate the immune response.

NLP-27 is required for fast paralysis of *C. elegans* and is independent of the MAP kinase PMK-1

To determine the function of NLP-27 during fungal infection, we generated *C. elegans nlp-27(rfl1)* mutant using CRISPR/Cas9 and deleted a 397 bp fragment (Figure 3A). To confirm the deletion, we used primers JEP965 and JEP966 in a qPCR (Figure 3B). In virulence assays, we found an increased paralysis time - which is the time it takes for *C. elegans* to stop moving after being trapped - in the *nlp-27(rfl1)* mutant as compared to wild type (Figure 3C). This was also confirmed by the paralysis time of worms treated with *nlp-27* RNAi (Figure S4). In comparison to the upregulation of *nlp-27* during *A. flagrans* infection, bacterial infections with *P. aeruginosa*, *S. marcescens*, *Enterococcus faecalis*, *Bacillus thuringiensis*, and *Photorhabdus luminescens* cause downregulation of *nlp-27*.[12,13] The lifespan of *C. elegans* was not changed by *nlp-27*

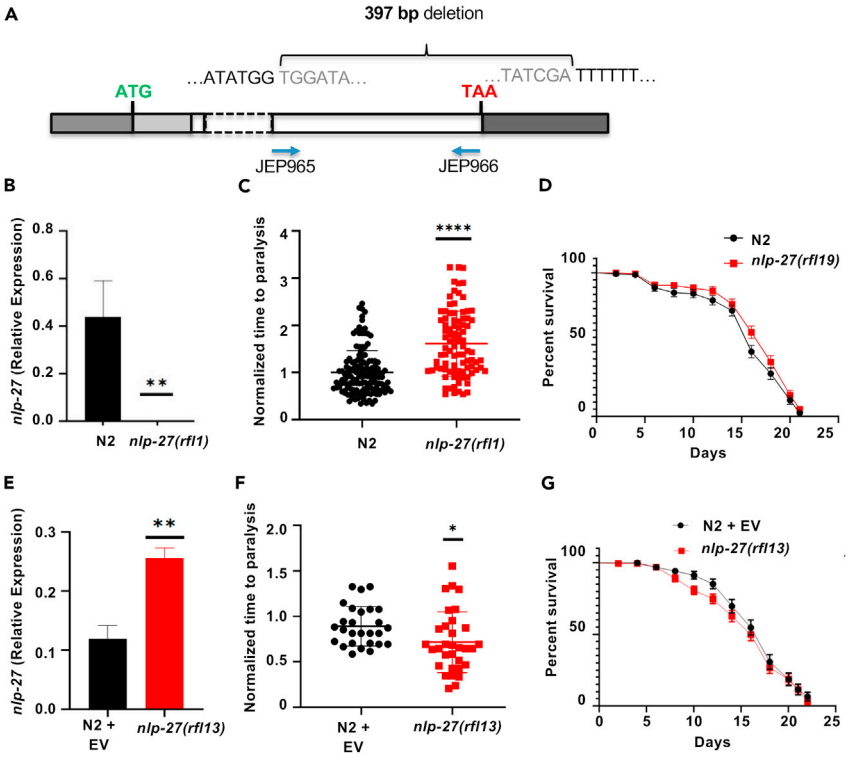

Figure 3. NLP-27 is required for fast paralysis during fungal infection

(A) Scheme of the *nlp-27*-deletion mutant *nlp-27(rfl1)*. Dark gray boxes represent the promoter region and the 3′ UTR, the light gray box represents the signal peptide, the white box represents the first exon and the dashed box the intron region.

(B) *nlp-27* relative expression in wild type *C. elegans* (N2) and the *nlp-27*-deletion strain *nlp-27(rfl1)*, **p < 0.01.

(C) Infection assay of N2 and the *nlp-27* deletion strain *nlp-27(rfl1)* with *A. flagrans*. ****p < 0.0001.

(D) Lifespan assays of N2 and the *nlp-27*-deletion strain *nlp-27(rfl1)*.

(E) NLP-27 overexpression in N2. *nlp-27* mRNA fold change in *nlp-27(rfl13)* overexpressing *nlp-27* under the native promoter relative to N2. **p < 0.01.

(F) Time to paralysis of N2 and the *nlp-27(rfl13)* strain. *p < 0.05.

(G) Lifespan assays of N2 and the *nlp-27(rfl13)* strain overexpressing *nlp-27* under *nlp-27* promoter in N2. Lifespans were performed in triplicates with at least 50 nematodes per replicate. Relative expression (2-ΔCt) is presented for each condition. *act-1* was used to normalize the Ct value of the genes. The mRNA fold change was calculated as a ratio of the relative expression of the condition tested to the control. Unpaired Student's t test was calculated for all experiments. ns p > 0.05, *p < 0.05, **p < 0.01, ***p < 0.001. Error bars represent SD.

deletion (Figure 3D). To further prove a function of NLP-27 in the paralysis process, we overexpressed *nlp-27* in wild-type *nlp-27(rfl13)* strain and in the *nlp-27* mutant strain *nlp-27(rfl6)*. The construct was obtained by amplifying 1.5 kb upstream of the coding region and 0.3 kb downstream of the coding region. Overexpression was demonstrated by qRT-PCR (Figure 3E). The paralysis time was reduced compared to the empty vector control (Figure 3F) verifying a role of NLP-27 in the infection. The lifespan was also unaffected after overexpression (Figure 3G). All the mutants showed normal motor phenotypes.

nlp-27 is part of the *nlp-29* cluster that was described to be under the control of the PMK-1 MAPK and the STA-2 transcription factor. Most data about the *nlp-29* cluster were obtained using *nlp-29* gene reporter strains, whose characteristics were then inferred to the whole cluster. To test whether this regulatory pathway was indeed involved in the case of the *nlp-27* gene, an infection assay was performed using the wild type and the *pmk-1*(*km25*) and *sta-2*(*ok1860*) mutants.[9] *nlp-27* expression in infection with *A. flagrans* was *pmk-1* and *sta-2* independent (Figure 4A). Hence, the pathway that regulates *nlp-27* expression differs from the pathway for *nlp-29* gene expression.[5,14]

nlp-27 expression is DCAR-1 dependent but independent of the human TRIB1 homolog NIPI-3

After wounding, the *C. elegans* immune system responds by initiating repair mechanisms and also upregulating AMPs like the *nlp-29* cluster.[14] NIPI-3 (no induction of peptide after *Drechmeria* infection) is a homolog of the human TRIB1 (tribbles homolog 1) and was identified upstream of SEK-1 (MAP2K). *nipi-3(fr4)* mutants respond to wounding by upregulating *nlp-29* expression, while during infection with *D. coniospora* there is no upregulation of *nlp-29*.[34] To determine if *nlp-27* induction depends on *nipi-3* in infection with *A. flagrans*, synchronized young adults of the mutant strain were infected in a 4 h assay as described previously. *nlp-27* expression was independent of *nipi-3* (Figure 4B). This indicates that *A. flagrans* and *D. coniospora* fungal infections induce different immune response pathways.

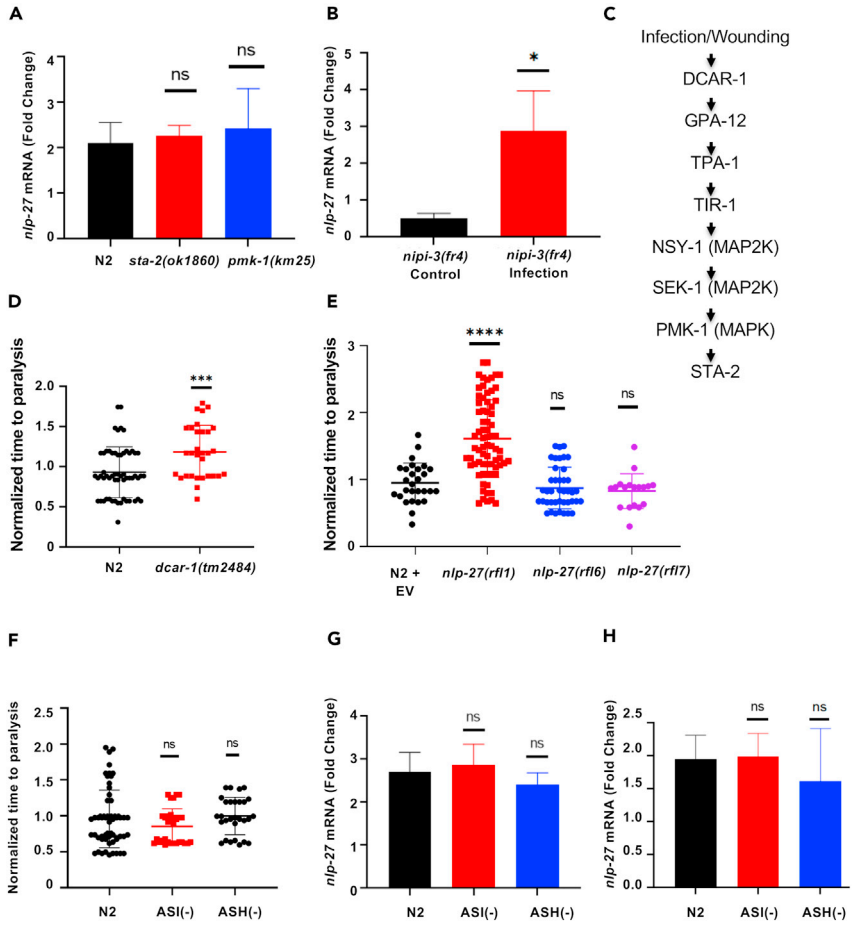

Figure 4. Expression analysis of *nlp-27*

(A) *nlp-27* relative expression in the *pmk-1(km25)* mutant and *sta-2(ok1860)* mutant. RNA was extracted from mutant strains after 4 h of co-incubation with induced *A. flagrans*, ns $p > 0.05$.

(B) *nlp-27* expression in a *nipi-3(fr4)* mutant background, *$p < 0.05$.

(C) Scheme of the PMK-1/p38 MAPK cascade activated by wounding or infection with *D. coniospora*.

(D) Time to paralysis of the *dcar-1(tm2484)*, ***$p < 0.001$.

(E) *nlp-27* complementation with *nlp-27* expressed under the native promoter *nlp-27(rfl6)* and under the hypodermal promoter *col-12 nlp-27(rfl7)*, ***$p < 0.001$.

(F) Time needed to paralyze the ASI(−) and ASH(−) ablated strains, ns $p > 0.05$.

(G) *nlp-27* mRNA fold change in infection with *A. flagrans* in the ASI(−) and ASH(−) ablated strains, ns $p > 0.05$.

(H) *nlp-27* mRNA fold change after exposure to 5 mM DHCA in the ASI(−) and ASH(−) ablated strains. For the virulence assays unpaired Student's t test was calculated for all experiments. ns $p > 0.05$, *$p < 0.05$, **$p < 0.01$, ***$p < 0.001$. Fold change was calculated as the relative expression ($2^{-\Delta Ct}$) ratio of the infected condition to the control condition for each strain in biological triplicates. Error bars represent sd. *act-1* was used to normalize the Ct value of the genes.

Because DCAR-1 is the known GPCR upstream of the *nlp-29* cluster[25] (Figure 4C), including *nlp-27*, we tested whether the *dcar-1(tm2484)* mutant behaves similar to the *nlp-27* mutant during infection. Indeed, *dcar-1(tm2484)* showed the same increased paralysis time as the *nlp-27* mutant when infected with *A. flagrans* (Figure 4D), confirming the relationship between *nlp-27* and DCAR-1. Moreover, the *nlp-27* mRNA fold change in *dcar-1(tm2484)* mutants in infection is lower than the fold change seen in the wild type during infection (Figure S5). All the mutants showed normal motor phenotypes.

Hypodermal expression of *nlp-27* rescues the paralysis phenotype

To determine if hypodermal or neuronal expression of *nlp-27* is required to rescue the paralysis phenotype of the *nlp-27* mutant, we expressed the *nlp-27* ORF in the mutant background under the hypodermal specific promoter *col-12* promoter as an extrachromosomal array in *nlp-27(rfl7)* (Figure S6A). The paralysis time of the transgenic strain resembled the time in wild type, suggesting that hypodermal expression is sufficient to explain the observed phenotype and that neuronal expression of *nlp-27* in ASI and ASH neurons might play an additional role other than paralysis (Figure 4E). Moreover, overexpression of *nlp-27* under the control of *col-12* showed a decreased paralysis time (Figure S6B). ASI(−) (PY7505) and ASH(−) (JN1713) strains express caspase in these pairs of neurons with help of specific promoters and both

showed the same paralysis phenotype as the wild type (Figure 4F).[29,35] The two neuronal ablated strains had also no significant change in the regulation of *nlp-27* compared to the control during infection with *A. flagrans*. This experiment showed that there is no involvement of the ASI and ASH neurons in *nlp-27* regulation during infection (Figure 4G). All the mutants showed normal motor phenotypes.

DCAR-1 is expressed in both ASI and ASH neurons and has been shown to be involved in the upregulation of *nlp-27* expression when *C. elegans* is exposed to dihydrocaffeic acid (DHCA).[25] ASH(−) and ASI(−) ablated strains showed the same upregulation of *nlp-27* after exposure to 5 mM DHCA similar to wild type (N2), suggesting that *nlp-27* expression is not modulated by either ASH or ASI neurons when the nematode is exposed to DHCA (Figure 4H).

A. flagrans causes dendrite degeneration of the PVD mechanosensory neurons close to the infection site

C. elegans has many natural pathogens and there have been reports that exposure to some pathogens like *P. aeruginosa* or *Streptomyces venezuelae* can cause neurodegeneration.[36,37] PVD neurons have ordered dendritic branches called menorahs and respond to harsh touch. The neurons are located between the hypodermis and its basement membrane.[38] The PVD neurons form a network of branches that envelop the body and tail of the nematode (Figure 5A). To investigate if *A. flagrans* infection can cause PVD neurodegeneration, the NC1686 *C. elegans* strain, where PVD neurons are visualized by GFP, was used in a fungal infection assay (Figure 5). When the neurons are intact, they appear as line-like structures (Figure 5A). The neurodegeneration phenotype is characterized by bead-like GFP structures along the neurons (Figure 5B). Synchronized NC1686 young adults were infected with *A. flagrans* and observed shortly after trapping. Neurodegeneration was indeed observed and seemed to spread from the trap site (Figures 5C–5E). The observed neurodegeneration in infection was quantified in Figure S7. To compare this observation with the neurodegeneration of the *nlp-27* mutants during infection we crossed the NC1686 strain with *nlp-27(rfl1)* mutants and obtained the line *nlp-27(rfl19)*. The *nlp-27* mutants *nlp-27(rfl19)* showed reduced neurodegeneration during infection as compared to the wild type but more neurodegeneration than non-infected nematodes. Nematodes trapped in the head area clearly had different degrees of neurodegeneration along the length of the nematode (Figure 5D). Sterile wounding also caused neurodegeneration (Figure S8).

NLP-27 causes dendrite neurodegeneration

We have shown that *A. flagrans* infection causes *nlp-29*-cluster gene upregulation. NLP-29 was shown to cause dendrite neurodegeneration in PVD neurons, whereas NLP-31—which is also similar to NLP-29—caused no dendrite neurodegeneration.[8] Therefore, we tested such a function for NLP-27. *nlp-27* was overexpressed in the NC1686 strain. A nematode was considered to have neurodegeneration if a total of ten or more bead structures were observed in more than five menorahs. NLP-27 expression led to neurodegeneration to a similar degree as NLP-29 (Figure 6A).

A processed NLP-27 fragment is sufficient to induce neurodegeneration

In *C. elegans* as in other animals, neuropeptides are typically derived from preproteins that undergo post-translational processing and modifications to yield mature neuropeptides. Mammal precursor molecules can be selectively processed to yield different peptides depending on the cell type.[39] Neuropeptide cleavage sites can be predicted using tools such as NeuroPred.[40] NLP-27 was predicted to be cleaved twice, once at the signal peptide site and once in the middle of the remaining peptide (Figure 6B).

To elucidate which fragment of the peptide is responsible for the neurodegeneration of the PVD neurons, two plasmids were constructed containing the signal peptide region and the first cleaved region (NLP-27A) or the signal peptide region and the second segment after the predicted cleavage (NLP-27B). The plasmids were injected in the NC1686 *C. elegans* line with GFP tagged PVD neurons and observed in the second and third day of adulthood. All the mutants showed normal motor phenotypes. We confirmed *nlp-27A* and *nlp-27B* expression in the strains expressing these fragments, *nlp-27A(rfl17)* and *nlp-27B(rfl18)*(Figure S9A). The strain expressing NLP-27A showed a higher level of degeneration in comparison to NLP-27B. Hence, NLP-27A appears to mainly be responsible for the neurodegeneration phenotype (Figure 6C) while expressing *nlp-27B* in the wild-type background seems to lead to a lower time to paralysis than overexpressing *nlp-27* (Figure S9B).

Next, we tested if Neprilypsin 1 (NEP-1), a membrane-bound metallopeptidase and a homolog of human enkephalinase is required for NLP-27 processing and control of the paralysis time.[4,41] However, a *C. elegans nep-1* mutant had a paralysis time similar to N2 in infection with *A. flagrans* (Figure 6D).

Opioid antagonist treated worms phenocopy *nlp-27* overexpression

NLP-27 contains the same YGGYG sequence motif as NLP-24, which binds the human μ and κ-type opioid receptors[41] (Figure 6E). In humans, opioid use alters the sleep architecture and causes a lack of sleep by decreasing the levels of adenosine, an endogenous somnogen.[42] These observations suggest that YGGYG containing peptides might have a role in the nematode opioid system. The opioid agonist morphine causes addiction-like behaviors in *C. elegans* while naloxone, an opioid antagonist, induces withdrawal symptoms.[43] To test if opioid antagonists have any effect on the paralysis time upon infection, synchronized young adults were treated with 10 mM naloxone by transferring them on LNA containing naloxone 10 mM for 4 h before the start of the virulence assay. Naloxone-treated nematodes behaved like the *nlp-27* overexpression strain (Figure 6F). Whether naloxone effect is additive to *nlp-27* overexpression or if naloxone is altering the time to paralysis of *nlp-27* mutant should be part of a follow-up study.

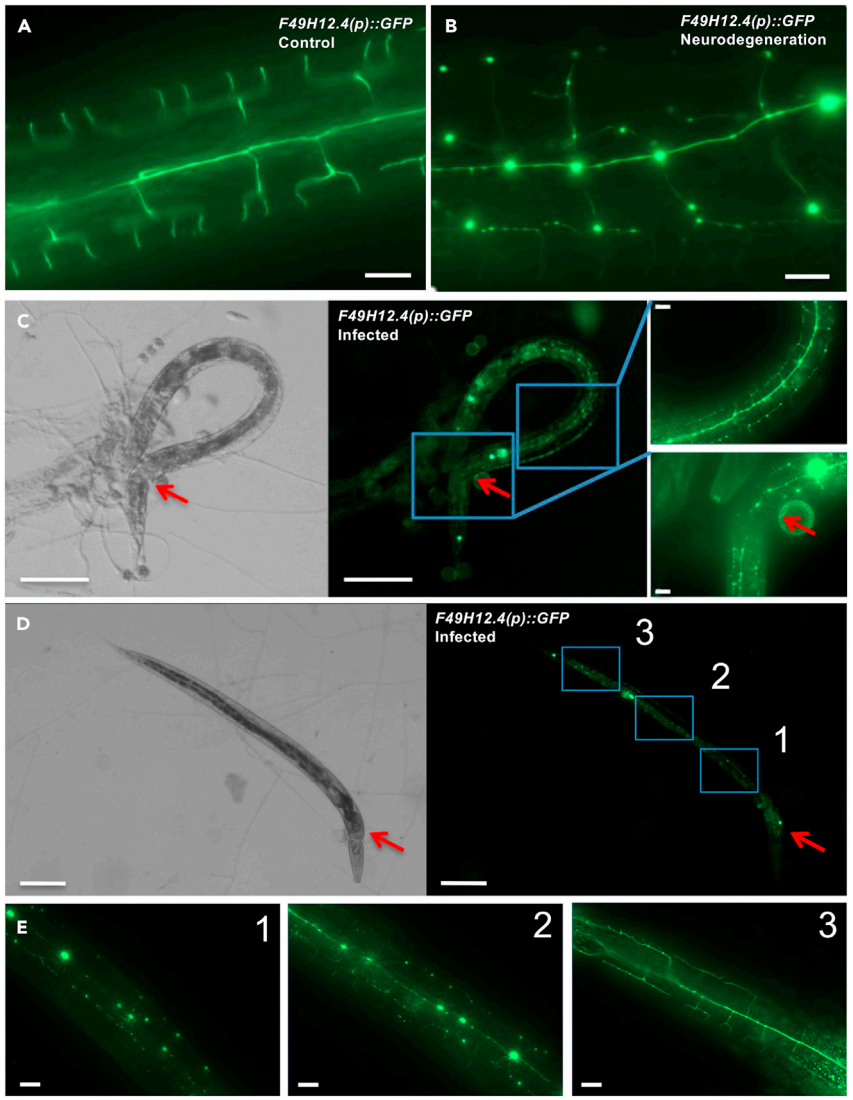

Figure 5. Neurodegeneration during *A. flagrans* infection

(A) Control PVD neurons in NC1686 expressing *F49H12.4(p)::GFP*. The scale bar represents 10 μm.

(B) Neurodegeneration of PVD neurons in NC1686 strain expressing *F49H12.4(p)::GFP*. The scale bar represents 10 μm.

(C) *C. elegans* NC1686 infected with *A. flagrans*. The arrows indicate the site of infection. The scale bar represents 100 μm.

(D) *C. elegans* NC1686 infected with *A. flagrans*. The arrows indicate the site of infection. The scale bar represents 100 μm.

(E) 1–3 are close ups from the regions indicated in (D). The scale bar represents 10 μm.

DISCUSSION

Neuropeptide-like proteins are widespread in eukaryotes but yet not well studied. However, their roles extend beyond neuronal tissues. *C. elegans* encodes over 48 precursor *nlp* genes,[44] and here we studied one member of the *nlp-29* gene cluster, *nlp-27*. All *nlp-29* cluster genes were upregulated upon infection with the nematode-trapping fungus *A. flagrans*, and *nlp-27* showed an interesting spatial expression pattern. *nlp-27* was downregulated at the infection site but upregulated in the head region and specifically in two neurons.

The upregulation of *nlp-27* after *A. flagrans* infection is in contrast to the effect during bacterial infections, where *nlp-27* is downregulated. The induction of *nlp-27* in the head region and the ASI and ASH neurons suggests a regulatory rather than an antimicrobial function since this expression is independent of the site of pathogen infection. Indeed, *nlp-27* upregulation decreased the paralysis time during the infection while *nlp-27*-deletion mutants had a longer paralysis time. Hence, upregulation of *nlp-27* appears advantageous for the success of *A. flagrans* and NLP-27 can be considered as an endogenous virulence factor. It is tempting to speculate that *A. flagrans* would have evolved mechanisms to prevent *nlp-27* upregulation if upregulation would have a negative effect.

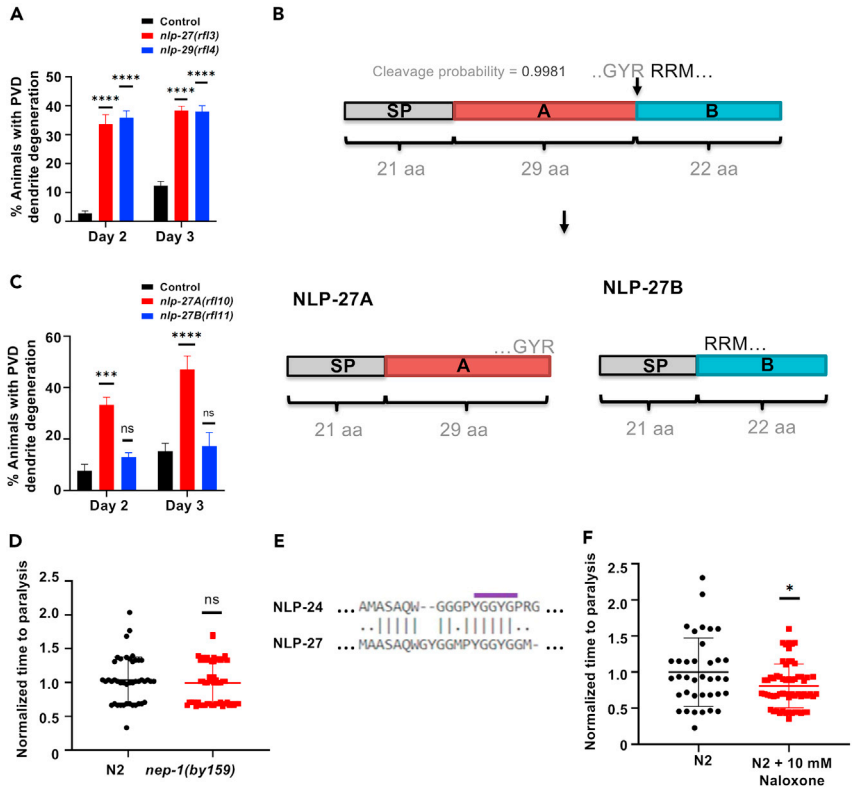

Figure 6. NLP-27 processing

(A) Percentage of NC1686 nematodes with PVD dendrite degeneration expressing empty-vector control (black), *nlp-27* (red), *nlp-27(rfl3)*, or *nlp-29* (blue) *nlp-29(rfl4)*. ****p < 0.0001. One-way ANOVA test was calculated.

(B) Scheme of NLP-27 with a cleavage site predicted with the NeuroCS prediction tool and Phobius.[50,51] The gray box represents the signal peptide, the red box peptide A and the blue box peptide B. Peptide A and peptide B were each fused to the SP for expression of the individual peptides in (C).

(C) Percentage of NC1686 nematodes with PVD dendrite degeneration expressing empty-vector control (black), *nlp-27*A (red) (strain *nlp-27(rfl10)*), *nlp-27*B (blue) (strain *nlp-27(rfl11)*). ns p > 0.5, ***p < 0.001, ****p < 0.0001. A one-way ANOVA test was applied.

(D) Time to paralysis of the *nep-1(by159)* mutant, ns p > 0.05.

(E) COBALT alignment of NLP-24 and NLP-27 with the YGGYG motif marked.[52]

(F) Time to paralysis of wild type *C. elegans* exposed to 10 mM naloxone for 4 h before the virulence assay. *p < 0.05. The unpaired Student's t test was applied.

In *C. elegans* there are two states of sleep, developmentally timed sleep (DTS) and stress-induced sleep (SIS). DTS occurs for 2–3 h between the larval stages and is dependent on the GABAergic RIS interneuron and the glutamatergic RIA interneurons.[45] SIS occurs after exposure to stimuli that cause cellular stress and is dependent on the peptidergic interneuron ALA.[46] If the sleep-like behavior during *A. flagrans* attack depends on one of the several sleep interneurons described in SIS and DTS remains to be determined. Here we showed the effect on sleep of NLP-27 in fungal infection. Perhaps the cuticle wounding during the fungal infection along with SSPs function to locally and systemically increase the production of NLPs, which in turn might act in a manner similar to that of the pro-inflammatory cytokines from mammals and the nemuri protein of *D. melanogaster*.[47] Overexpression of *nlp-27* decreased the time of paralysis after infection, suggesting the fungus may benefit from the nematode immune response. A shorter paralysis time translates into faster availability of nutrients for the fungus and less chances for *C. elegans* to escape or rupture the mycelium. In humans, opioid use alters the sleep architecture and causes a lack of sleep by decreasing the levels of adenosine, an endogenous somnogen.[42] Perhaps the sleep induction seen in the case of *nlp-27* overexpression has an opioid antagonistic effect and promotes sleep to increase the survival chances of the nematode.[11]

In contrast, *nlp-31* is slightly upregulated in bacterial infection with *B. thuringiensis* and *P. aeruginosa* while *nlp-29* has the same expression pattern as *nlp-27*.[12] All three genes are expressed in the hypodermis while *nlp-27* is also localized in some neurons. During infection, only *nlp-29* expression is increased at the infection site while *nlp-27* expression increases in the head area and *nlp-31* is induced everywhere. A stark difference between the three peptides is their signaling cascades. Both *nlp-31* and *nlp-29* are *pmk-1* and *sta-2* dependent while *nlp-27* expression is independent of both. However, the *nlp-27* promoter region contains two binding sites for the transcription factor DAF-16 (CTTATCA) suggesting that *nlp-27* transcription might be regulated via DAF-16 in a DAF-2 dependent manner. We have checked the expression of *nlp-27* in DAF-2 mutants (unpublished results), but we have not noticed any significant regulation during infection with *A. flagrans* in the expression of

nlp-27. Therefore, these three members of the *nlp-29*-cluster display high sequence similarities but their expression in infection suggests overlapping and distinct roles.

Expression of *nlp-27* in ASI and ASH neurons indicates a complex chemosensory regulation of the gene in both neurons. However, it is not yet clear whether ASH and ASI detect the pathogens directly or whether they get the signal from other sensory neurons. Exposure to dihydrocaffeic acid (DHCA) upregulates the expression of *nlp-27* in a DCAR-1 dependent manner. The ASH(−) and ASI(−) neuronal ablated strain showed similar *nlp-27* expression to wild type (N2) when exposed to 5 mM DHCA. Interestingly, *nlp-27* expression in the hypodermis alone was sufficient to induce a longer paralysis phenotype, suggesting that neuronal expression of *nlp-27* might play an additional role. Moreover, *nlp-27* is not dependent on PMK-1 and STA-2 like other *nlp-29*-cluster genes, suggesting that NLP-27 acts in a distinct manner.

Trapped nematodes showed a neurodegeneration gradient from the trap site along the length of the nematode. Interestingly, wounding alone also caused PVD neurodegeneration. Therefore, fungal infection probably causes neurodegeneration through the wounding response. Perhaps neurodegeneration is an effect of any innate immune response, and this only proves again the fact that *A. flagrans* wounds the worm and triggers an innate immune response. Since *nlp-29* was upregulated in the area of trap formation, it is likely that mainly high concentrations of NLP-29 cause the observed neurodegeneration gradient. However, NLP-27 also enhanced neurodegeneration upon infection. This might be especially important further away from the infection site, where NLP-27 could be the main player. Taken together, *A. flagrans* apparently induces NLP-27 and NLP-29 to enhance neurodegeneration. Hence, both neuropeptides can be considered as endogenous virulence factors.

NLP-27 is predicted to contain a neuropeptide cleavage site, and indeed one of the predicted peptide fragments was able to induce neurodegeneration as NLP-27 full length. NLP-24, a peptide from the same YGGYG family as NLP-27, is processed into opioid-like peptides to activate neuropeptide receptor 17 (NPR-17). The YGGYG peptide also activated the human κ and μ opioid receptors in a cell culture.[41] NLP-27 might also be processed in an opioid-specific manner. A candidate for the processing was *C. elegans* NEP-1, a homolog of human enkephalinase.[41] The fact that the paralysis time of *nep-1* mutant strains was not different from wild type suggests that either NEP-1 has no function in NLP-27 activation or that the NLP-27 full-length peptide is also biologically active. Another possibility is that NLP-27, or the N-terminal fragment thereof, is not further processed and YGGYG released, but that the protein motif binds to the receptor and blocks the ligand-binding site. This can also be inferred from the fact that naloxone phenocopies the effect of NLP-27 overexpression. Hence, the effect of NLP-27 induction in *C. elegans* resembles the effect of pro-inflammatory cytokines such as interleukin-1 and tumor necrosis factor–α in humans. These cytokines promote sleep by altering the excitability of sleep-inducing neurons.[48,49] The next step should be to identify the GPCR responsible for NLP-27 peptide binding. The fact that the ASI ablation strain did not show any difference in the paralysis time speaks against NPR-17 (the NLP-24 receptor) because NPR-17 should be expressed in those neurons. Also, creating a non-cleavable NLP-27 to determine whether cleavage is necessary for the observed phenotypes is an interesting aspect and should be observed in a follow-up study.

Studying the effect of infection on the release of neuropeptides will contribute to the understanding of the mechanism by which the fungus overcomes the host defense and kills the nematode, as well as the effects of the neuropeptides in the host organism during an infectious attack. The inflammatory host immune response and its connection to the opioid-like processing is of importance as peptide-GPCR binding relationships are highly conserved across animals and modulating this response can modulate the inflammatory response. This work has shed light on the function of NLPs in general and how they perhaps may act as endogenous opioid receptor antagonists.

Limitations of the study

We show that NLP-27 is upregulated during fungal attack. However, it is also upregulated upon wounding, and it remains open if specific fungal signals add to the induction. We also discovered that the N-terminal fragment of NLP-27 is sufficient to induce neurodegeneration but that the C-terminal part reduced the time to paralysis. Although it is tempting to speculate that the YGGYG motifs within the fragment are the active entities and that the peptide is processed into the fragments A and B or even further, it remains to be determined if neuropeptide processing occurs indeed during the infection. Additionally, our findings indicate that nematodes exposed to naloxone, an opioid receptor antagonist, behave similar to nematodes overexpressing *nlp-27*. Future research is necessary to test whether NLP-27 functions in a manner similar to an opioid antagonist and whether it binds to an opioid receptor.

STAR★METHODS

Detailed methods are provided in the online version of this paper and include the following:

- KEY RESOURCES TABLE
- RESOURCE AVAILABILITY
  - Lead contact
  - Materials availability
  - Data and code availability
- EXPERIMENTAL MODEL AND STUDY PARTICIPANT DETAILS
- METHOD DETAILS

- qRT-PCR
- CRISPR/Cas9 knock-out
- Cultivation of *A. flagrans*
- *C. elegans* infection assay
- *C. elegans* virulence assay
- *C. elegans* lifespan
- *C. elegans* PVD dendrite degeneration quantification
- *C. elegans* sterile wounding
- *C. elegans* amphid neurons staining with DiO
- RNAi treatment

● QUANTIFICATION AND STATISTICAL ANALYSIS

SUPPLEMENTAL INFORMATION

Supplemental information can be found online at https://doi.org/10.1016/j.isci.2024.109484.

ACKNOWLEDGMENTS

This work was supported by the Deutsche Forschungsgemeinschaft (DFG Fi 459-26/1). Some strains used in this study were provided by the Caenorhabditis Genetics Center (CGC), which is funded by the NIH Office of Research Infrastructure Programs (P40 OD010440). We thank Dr. Sotiris Amillis for critically reviewing the manuscript.

AUTHOR CONTRIBUTIONS

M.P. performed most of the experiments. Conceptualization, M.P. and R.F.; methodology and investigation, M.P., A.-L.K., L.S., P.L.S., V.B.; E.W. (all *C. elegans* injections), writing – original draft, M.P.; writing – review and editing, R.F.; resources, R.F.; supervision, N.W. and R.F.

DECLARATION OF INTERESTS

The authors declare no competing interests.

Received: March 2, 2023
Revised: October 26, 2023
Accepted: March 8, 2024
Published: March 12, 2024

REFERENCES

1. Procaccini, C., Pucino, V., De Rosa, V., Marone, G., and Matarese, G. (2014). Neuro-endocrine networks controlling immune system in health and disease. Front. Immunol. *5*, 143. https://doi.org/10.3389/fimmu.2014.00143.
2. McKay, F.M., McCoy, C.J., Crooks, B., Marks, N.J., Maule, A.G., Atkinson, L.E., and Mousley, A. (2022). In silico analyses of neuropeptide-like protein (NLP) profiles in parasitic nematodes. Int. J. Parasitol. *52*, 77–85. https://doi.org/10.1016/j.ijpara.2021.07.002.
3. Nathoo, A.N., Moeller, R.A., Westlund, B.A., and Hart, A.C. (2001). Identification of neuropeptide-like protein gene families in *Caenorhabditis elegans* and other species. Proc. Natl. Acad. Sci. USA *98*, 14000–14005. https://doi.org/10.1073/pnas.241231298.
4. Li, C., and Kim, K. (2008). Neuropeptides. In WormBook, pp. 1–36. https://doi.org/10.1895/wormbook.1.142.1.
5. Couillault, C., Pujol, N., Reboul, J., Sabatier, L., Guichou, J.F., Kohara, Y., and Ewbank, J.J. (2004). TLR-independent control of innate immunity in *Caenorhabditis elegans* by the TIR domain adaptor protein TIR-1, an ortholog of human SARM. Nat. Immunol. *5*, 488–494. https://doi.org/10.1038/ni1060.
6. Hickman, S.E., Kingery, N.D., Ohsumi, T.K., Borowsky, M.L., Wang, L.C., Means, T.K., and El Khoury, J. (2013). The microglial sensome revealed by direct RNA sequencing. Nat. Neurosci. *16*, 1896–1905. https://doi.org/10.1038/nn.3554.
7. Frakes, A.E., Metcalf, M.G., Tronnes, S.U., Bar-Ziv, R., Durieux, J., Gildea, H.K., Kandahari, N., Monshietehadi, S., and Dillin, A. (2020). Four glial cells regulate ER stress resistance and longevity via neuropeptide signaling in *C. elegans*. Science *367*, 436–440. https://doi.org/10.1126/science.aaz6896.
8. E, L., Zhou, T., Koh, S., Chuang, M., Sharma, R., Pujol, N., Chisholm, A.D., Eroglu, C., Matsunami, H., and Yan, D. (2018). An antimicrobial peptide and its neuronal receptor regulate dendrite degeneration in aging and infection. Neuron *97*, 125–138.e5. https://doi.org/10.1016/j.neuron.2017.12.001.
9. Dierking, K., Polanowska, J., Omi, S., Engelmann, I., Gut, M., Lembo, F., Ewbank, J.J., and Pujol, N. (2011). Unusual regulation of a STAT protein by an SLC6 family transporter in *C. elegans* epidermal innate immunity. Cell Host Microbe *9*, 425–435. https://doi.org/10.1016/j.chom.2011.04.011.
10. Albeg, A., Smith, C.J., Chatzigeorgiou, M., Feitelson, D.G., Hall, D.H., Schafer, W.R., Miller, D.M., 3rd, and Treinin, M. (2011). *C. elegans* multi-dendritic sensory neurons: morphology and function. Mol. Cell. Neurosci. *46*, 308–317. https://doi.org/10.1016/j.mcn.2010.10.001.
11. Sinner, M.P., Masurat, F., Ewbank, J.J., Pujol, N., and Bringmann, H. (2021). Innate immunity promotes sleep through epidermal antimicrobial peptides. Curr. Biol. *31*, 564–577.e12. https://doi.org/10.1016/j.cub.2020.10.076.
12. Nakad, R., Snoek, L.B., Yang, W., Ellendt, S., Schneider, F., Mohr, T.G., Rösingh, L., Masche, A.C., Rosenstiel, P.C., Dierking, K., et al. (2016). Contrasting invertebrate immune defense behaviors caused by a single gene, the *Caenorhabditis elegans* neuropeptide receptor gene *npr-1*. BMC Genom. *17*, 280. https://doi.org/10.1186/s12864-016-2603-8.
13. Engelmann, I., Griffon, A., Tichit, L., Montañana-Sanchis, F., Wang, G., Reinke, V., Waterston, R.H., Hillier, L.W., and Ewbank, J.J. (2011). A comprehensive analysis of gene expression changes provoked by bacterial and fungal infection in *C. elegans*. PLoS One *6*, e19055. https://doi.org/10.1371/journal.pone.0019055.
14. Pujol, N., Zugasti, O., Wong, D., Couillault, C., Kurz, C.L., Schulenburg, H., and Ewbank,

J.J. (2008). Anti-fungal innate immunity in *C. elegans* is enhanced by evolutionary diversification of antimicrobial peptides. PLoS Pathog. *4*, e1000105. https://doi.org/10.1371/journal.ppat.1000105.
15. Jiang, X., Xiang, M., and Liu, X. (2017). Nematode-trapping fungi. Microbiol. Spectr. *5*. https://doi.org/10.1128/microbiolspec.FUNK-0022-2016.
16. Fischer, R., and Requena, N. (2022). Small secreted proteins as virulence factors in nematode-trapping fungi. Trends Microbiol. *30*, 615–617.
17. Hsueh, Y.P., Gronquist, M.R., Schwarz, E.M., Nath, R.D., Lee, C.H., Gharib, S., Schroeder, F.C., and Sternberg, P.W. (2017). Nematophagous fungus *Arthrobotrys oligospora* mimics olfactory cues of sex and food to lure its nematode prey. Elife *6*, e20023. https://doi.org/10.7554/eLife.20023.
18. Hsueh, Y.P., Mahanti, P., Schroeder, F.C., and Sternberg, P.W. (2013). Nematode-trapping fungi eavesdrop on nematode pheromones. Curr. Biol. *23*, 83–86. https://doi.org/10.1016/j.cub.2012.11.035.
19. Yu, X., Hu, X., Pop, M., Wernet, N., Kirschhöfer, F., Brenner-Weiß, G., Keller, J., Bunzel, M., and Fischer, R. (2021). Fatal attraction of *Caenorhabditis elegans* to predatory fungi through 6-methyl-salicylic acid. Nat. Commun. *12*, 5462.
20. Hammadeh, H.H., Serrano, A., Wernet, V., Stomberg, N., Hellmeier, D., Weichert, M., Brandt, U., Sieg, B., Kanofsky, K., Hehl, R., et al. (2022). A dialog-like cell communication mechanism is conserved in filamentous ascomycete fungi and mediates interspecies interactions. Proc. Natl. Acad. Sci. USA *119*, e2112518119.
21. Wernet, V., Wäckerle, J., and Fischer, R. (2022). The STRIPAK component SipC is involved in morphology and cell-fate determination in the nematode-trapping fungus *Duddingtonia flagrans*. Genetics *220*, iyab153.
22. Wernet, N., Wernet, V., and Fischer, R. (2021). The small-secreted cysteine-rich protein CyrA is a virulence factor of *Duddingtonia flagrans* during the *Caenorhabditis elegans* attack. PLoS Pathog. *17*, e1010028.
23. Youssar, L., Wernet, V., Hensel, N., Yu, X., Hildebrand, H.-G., Schreckenberger, B., Kriegler, M., Hetzer, B., Frankino, P., Dillin, A., and Fischer, R. (2019). Intercellular communication is required for trap formation in the nematode-trapping fungus *Duddingtonia flagrans*. PLoS Genet. *15*, e1008029.
24. Aoki, R., Yagami, T., Sasakura, H., Ogura, K.I., Kajihara, Y., Ibi, M., Miyamae, T., Nakamura, F., Asakura, T., Kanai, Y., et al. (2011). A seven-transmembrane receptor that mediates avoidance response to dihydrocaffeic acid, a water-soluble repellent in *Caenorhabditis elegans*. J. Neurosci. *31*, 16603–16610. https://doi.org/10.1523/JNEUROSCI.4018-11.2011.
25. Zugasti, O., Bose, N., Squiban, B., Belougne, J., Kurz, C.L., Schroeder, F.C., Pujol, N., and Ewbank, J.J. (2014). Activation of a G protein-coupled receptor by its endogenous ligand triggers the innate immune response of *Caenorhabditis elegans*. Nat. Immunol. *15*, 833–838. https://doi.org/10.1038/ni.2957.
26. Hong, R.L., Riebesell, M., Bumbarger, D.J., Cook, S.J., Carstensen, H.R., Sarpolaki, T., Cochella, L., Castrejon, J., Moreno, E., Sieriebriennikov, B., et al. (2019). Evolution of neuronal anatomy and circuitry in two highly divergent nematode species. Elife *8*, e47155. https://doi.org/10.7554/eLife.47155.
27. Fielenbach, N., and Antebi, A. (2008). *C. elegans* dauer formation and the molecular basis of plasticity. Genes Dev. *22*, 2149–2165. https://doi.org/10.1101/gad.1701508.
28. White, J.Q., and Jorgensen, E.M. (2012). Sensation in a single neuron pair represses male behavior in hermaphrodites. Neuron *75*, 593–600. https://doi.org/10.1016/j.neuron.2012.03.044.
29. Beverly, M., Anbil, S., and Sengupta, P. (2011). Degeneracy and neuromodulation among thermosensory neurons contribute to robust thermosensory behaviors in *Caenorhabditis elegans*. J. Neurosci. *31*, 11718–11727. https://doi.org/10.1523/JNEUROSCI.1098-11.2011.
30. Chen, Z., Hendricks, M., Cornils, A., Maier, W., Alcedo, J., and Zhang, Y. (2013). Two insulin-like peptides antagonistically regulate aversive olfactory learning in *C. elegans*. Neuron *77*, 572–585. https://doi.org/10.1016/j.neuron.2012.11.025.
31. Hallem, E.A., Spencer, W.C., McWhirter, R.D., Zeller, G., Henz, S.R., Rätsch, G., Miller, D.M., 3rd, Horvitz, H.R., Sternberg, P.W., and Ringstad, N. (2011). Receptor-type guanylate cyclase is required for carbon dioxide sensation by *Caenorhabditis elegans*. Proc. Natl. Acad. Sci. USA *108*, 254–259. https://doi.org/10.1073/pnas.1017354108.
32. Cao, X., Kajino-Sakamoto, R., Doss, A., and Aballay, A. (2017). Distinct roles of sensory neurons in mediating pathogen avoidance and neuropeptide-dependent immune regulation. Cell Rep. *21*, 1442–1451. https://doi.org/10.1016/j.celrep.2017.10.050.
33. Khodakova, A., and Beloborodova, N. (2007). Microbial metabolites in the blood of patients with sepsis. Crit. Care *11*, P5.
34. Ziegler, K., Kurz, C.L., Cypowyj, S., Couillault, C., Pophillat, M., Pujol, N., and Ewbank, J.J. (2009). Antifungal innate immunity in *C. elegans*: PKCdelta links G protein signaling and a conserved p38 MAPK cascade. Cell Host Microbe *5*, 341–352. https://doi.org/10.1016/j.chom.2009.03.006.
35. Yoshida, K., Hirotsu, T., Tagawa, T., Oda, S., Wakabayashi, T., Iino, Y., and Ishihara, T. (2012). Odour concentration-dependent olfactory preference change in *C. elegans*. Nat. Commun. *3*, 739. https://doi.org/10.1038/ncomms1750.
36. Gravato-Nobre, M.J., Vaz, F., Filipe, S., Chalmers, R., and Hodgkin, J. (2016). The invertebrate lysozyme effector ILYS-3 is systemically activated in response to danger signals and confers antimicrobial protection in *C. elegans*. PLoS Pathog. *12*, e1005826. https://doi.org/10.1371/journal.ppat.1005826.
37. Caldwell, K.A., Tucci, M.L., Armagost, J., Hodges, T.W., Chen, J., Memon, S.B., Blalock, J.E., DeLeon, S.M., Findlay, R.H., Ruan, Q., et al. (2009). Investigating bacterial sources of toxicity as an environmental contributor to dopaminergic neurodegeneration. PLoS One *4*, e7227. https://doi.org/10.1371/journal.pone.0007227.
38. Yuval, O., Iosilevskii, Y., Meledin, A., Podbilewicz, B., and Shemesh, T. (2021). Neuron tracing and quantitative analyses of dendritic architecture reveal symmetrical three-way-junctions and phenotypes of git-1 in *C. elegans*. PLoS Comput. Biol. *17*, e1009185. https://doi.org/10.1371/journal.pcbi.1009185.
39. Salio, C., Lossi, L., Ferrini, F., and Merighi, A. (2006). Neuropeptides as synaptic transmitters. Cell Tissue Res. *326*, 583–598. https://doi.org/10.1007/s00441-006-0268-3.
40. Southey, B.R., Amare, A., Zimmerman, T.A., Rodriguez-Zas, S.L., and Sweedler, J.V. (2006). NeuroPred: a tool to predict cleavage sites in neuropeptide precursors and provide the masses of the resulting peptides. Nucleic Acids Res. *34*, W267–W272. https://doi.org/10.1093/nar/gkl161.
41. Cheong, M.C., Artyukhin, A.B., You, Y.J., and Avery, L. (2015). An opioid-like system regulating feeding behavior in *C. elegans*. Elife *4*, e06683. https://doi.org/10.7554/eLife.06683.
42. Moore, J.T., and Kelz, M.B. (2009). Opiates, sleep, and pain: the adenosinergic link. Anesthesiology *111*, 1175–1176. https://doi.org/10.1097/ALN.0b013e3181bdfa2e.
43. Ide, S., Kunitomo, H., Iino, Y., and Ikeda, K. (2021). *Caenorhabditis elegans* exhibits morphine addiction-like behavior via the opioid-like receptor NPR-17. Front. Pharmacol. *12*, 802701. https://doi.org/10.3389/fphar.2021.802701.
44. Frooninckx, L., Van Rompay, L., Temmerman, L., Van Sinay, E., Beets, I., Janssen, T., Husson, S.J., and Schoofs, L. (2012). Neuropeptide GPCRs in *C. elegans*. Front. Endocrinol. *3*, 167. https://doi.org/10.3389/fendo.2012.00167.
45. Turek, M., Lewandrowski, I., and Bringmann, H. (2013). An AP2 transcription factor is required for a sleep-active neuron to induce sleep-like quiescence in *C. elegans*. Curr. Biol. *23*, 2215–2223. https://doi.org/10.1016/j.cub.2013.09.028.
46. Van Buskirk, C., and Sternberg, P.W. (2007). Epidermal growth factor signaling induces behavioral quiescence in *Caenorhabditis elegans*. Nat. Neurosci. *10*, 1300–1307. https://doi.org/10.1038/nn1981.
47. Toda, H., Williams, J.A., Gulledge, M., and Sehgal, A. (2019). A sleep-inducing gene, nemuri, links sleep and immune function in Drosophila. Science *363*, 509–515. https://doi.org/10.1126/science.aat1650.
48. Majde, J.A., and Krueger, J.M. (2005). Links between the innate immune system and sleep. J. Allergy Clin. Immunol. *116*, 1188–1198. https://doi.org/10.1016/j.jaci.2005.08.005.
49. Zielinski, M.R., and Krueger, J.M. (2011). Sleep and innate immunity. Front. Biosci. *3*, 632–642. https://doi.org/10.2741/s176.
50. Wang, Y., Kang, J., Li, N., Zhou, Y., Tang, Z., He, B., and Huang, J. (2020). NeuroCS: A tool to predict cleavage sites of neuropeptide precursors. Protein Pept. Lett. *27*, 337–345. https://doi.org/10.2174/0929866526666191112150636.
51. Käll, L., Krogh, A., and Sonnhammer, E.L.L. (2007). Advantages of combined transmembrane topology and signal peptide prediction–the Phobius web server. Nucleic Acids Res. *35*, W429–W432. https://doi.org/10.1093/nar/gkm256.
52. Papadopoulos, J.S., and Agarwala, R. (2007). COBALT: constraint-based alignment tool for multiple protein sequences. Bioinformatics *23*, 1073–1079. https://doi.org/10.1093/bioinformatics/btm076.
53. Brenner, S. (1974). The genetics of Caenorhabditis elegans. Genetics *77*.
54. Pujol, N., Cypowyj, S., Ziegler, K., Millet, A., Astrain, A., Goncharov, A., Jin, Y.,

Chisholm, A.D., and Ewbank, J.J. (2008). Distinct innate immune responses to infection and wounding in the *C. elegans* epidermis. Curr. Biol. *18*, 481–489. https://doi.org/10.1016/j.cub.2008.02.079.

55. Zugasti, O., and Ewbank, J.J. (2009). Neuroimmune regulation of antimicrobial peptide expression by a noncanonical TGF-beta signaling pathway in *Caenorhabditis elegans* epidermis. Nat. Immunol. *10*, 249–256. https://doi.org/10.1038/ni.1700.
56. Zhang, Y., Chen, D., Smith, M.A., Zhang, B., and Pan, X. (2012). Selection of reliable reference genes in *Caenorhabditis elegans* for analysis of nanotoxicity. PLoS One *7*, e31849. https://doi.org/10.1371/journal.pone.0031849.
57. Zhang, L., Ward, J.D., Cheng, Z., and Dernburg, A.F. (2015). The auxin-inducible degradation (AID) system enables versatile conditional protein depletion in *C. elegans*. Development *142*, 4374–4384. https://doi.org/10.1242/dev.129635.
58. Schindelin, J., Arganda-Carreras, I., Frise, E., Kaynig, V., Longair, M., Pietzsch, T., Preibisch, S., Rueden, C., Saalfeld, S., Schmid, B., et al. (2012). Fiji: an open-source platform for biological-image analysis. Nat. Methods *9*, 676–682. https://doi.org/10.1038/nmeth.2019.

STAR★METHODS

KEY RESOURCES TABLE

REAGENT or RESOURCE	SOURCE	IDENTIFIER
Experimental models: Organisms/strains		
IG544, *nipi-3(fr4)*	Pujol et al.[54]	N/A
IG1241, *sta-2(ok1860)*	Dierking et al.[9]	N/A
KU25, *pmk-1*(km25)	Caenorhabditis Genetics Centre (CGC)	WB Strain: KU25; WormBase: WBVar00024040
PY7505, *oyIs84* [*gpa-4(p)::TU#813 + gcy-27(p)::TU#814 + gcy-27(p)::GFP + unc-122(p)::DsRed*]	Beverly et al.[29]	N/A
JN1713, peIs1713 [*sra-6(p)::mCasp-1 + unc-122(p)::mCherry*]	Yoshida et al.[35]	N/A
NC1686, *wdIs51 [F49H12.4(p)::GFP + unc-119(+)]*	Caenorhabditis Genetics Centre (CGC)	WB Strain: NC1686; WormBase: WBVar00028680
BR2815, *nep-1(by159)*	Caenorhabditis Genetics Centre (CGC)	WB Strain: BR2815; WormBase: WBVar00003896
YC307, *dcar-1(tm2484)*	Aoki et al.[24]	N/A
KIT24, *nlp-27(rfl1) + myo-2(p)::dTtomato*	This paper	N/A
KIT26, *rfl2* [*dcar-1(p)::NLS-GFP::unc-54 3′ UTR + nlp-27(p)::NLS-wrmScarlet::unc-54 3′ UTR + unc-119(+)*]	This paper	N/A
KIT27, *rfl3 [NC1686 + nlp-27(p)::nlp-27::nlp-27 3′ UTR + myo-2(p)::dTtomato*]	This paper	N/A
KIT28, *rfl4* [*NC1686 + nlp-29(p)::nlp-29::nlp-29 3′ UTR + myo-2(p) ::dTtomato*]	This paper	N/A
KIT29, *rfl5* [*nlp-29(p)::NLS-GFP::unc-54 3′ UTR + nlp-31(p)::NLS-wrmScarlet::unc-54 3′ UTR + unc-119(+)*]	This paper	N/A
KIT30, *rfl6 [KIT24 + nlp-27(p)::nlp-27:: nlp-27 3′ UTR + myo-2(p)::GFP]*	This paper	N/A
KIT31, *rfl7 [KIT24 + col-12(p)::nlp-27:: col-12 3′ UTR + myo-2(p)::GFP]*	This paper	N/A
KIT33, *rfl8 [N2 + nlp-27(p)::nlp-27-wrmScarlet:: nlp-27 3′ UTR + myo-2(p)::GFP]*	This paper	N/A
KIT35, *rfl10 [NC1686 + nlp-27(p)::nlp-27A:: nlp-27 3′ UTR + myo2(p)::dTtomato]*	This paper	N/A
KIT36, *rfl11 [NC1686 + nlp-27(p)::nlp-27B:: nlp-27 3′ UTR + myo2(p)::dTtomato]*	This paper	N/A
KIT37, *rfl12 [NC1686 + chill18(p)::NLS-wrmScarlet:: unc-54 3′ UTR + myo-2(p)::dTtomato]*	This paper	N/A
KIT38, *rfl13 [N2 + nlp-27p::nlp-27:: nlp-27 3′UTR + myo2(p)::dTtomato]*	This paper	N/A
KIT54, *rfl16 [N2+ col-12(p)::nlp-27:: col-12 3′UTR + myo2(p):: dTtomato]*	This paper	N/A
KIT55, *rfl17 [N2+ nlp-27(p)::nlp-27A:: nlp-27 3′ UTR + myo2(p)::dTtomato]*	This paper	N/A
KIT56, *rfl18 [N2+ nlp-27(p)::nlp-27B:: nlp-27 3′ UTR + myo2(p)::dTtomato]*	This paper	N/A
KIT60, *rfl19 [NC1686; nlp-27(rfl1)]*	This paper	N/A

(*Continued on next page*)

Continued

REAGENT or RESOURCE	SOURCE	IDENTIFIER
Oligonucleotides		
pVB01-FW, AGATATCCTGCAGGAATTCCTC GAGCAAAGTGGTGTTTTACAACATTATTG	This paper	N/A
pVB01-RV, TGCACTTATAATACGACTCACTA GTAAAGATCGAAAATTCATTATTATTTACAAAG	This paper	N/A
pVB02-FW, AGATATCCTGCAGGAATTCCTC GAGGAATGGAGTGCTTGTAAAAACATAC	This paper	N/A
pVB02-RV, TGCACTTATAATACGACTCACTAG TATGCAAGTTTTTATTCAAGAAAAAAGTGA	This paper	N/A
pMM15-FW, AGATATCCTGCAGGAATTCCTCGA GCCACATTGTAACTATTGAGTGAG	This paper	N/A
pMM15-RV, CACCTTACGCTTCTTCTTTGGCATAAT GATATTTCTTTGAAAAACTTGTAAATAA	This paper	N/A
pMM18-FW, TAACAATTTCACAGGGCCCCTCGAG TGTGCTCGTTTCAAAAATTTACAAA	This paper	N/A
pMM18-RV, AAGTGAAGAAGTGGAAATCATTTTT CTAAAAAGTAATCAAATCTTAGTAA	This paper	N/A
pMM18-FW-UTR, ACGGTGGATACGGTGGATGGG GAAAGTAAGCGCTTCAATGACATCTCATT	This paper	N/A
pMM18-RV-UTR, AAGTTGGGTAACGCCAGACTAG TATTTGTAATGAAATCATTTATTCCACT	This paper	N/A
pMM19-FW, AGATATCCTGCAGGAATTCCTCGAGC TTGTCAAAAAGTTTGTATTTCGGAT	This paper	N/A
pMM19-RV, TAAGAAGTGAAGAAGTGGAAATCATG GCAAAATCTGAAATAATAAATATTAAATTC	This paper	N/A
pMM19-FW-UTR, TGGATACGGTGGATGGGGAAA GTAATTGATGAGTCTGTTATTGTAGTTAA	This paper	N/A
pMM19-RV-UTR, TAAGTTGGGTAACGCCAGACTA GTTTTTCATTGTAAAATTTTTCATTAAAAACAT	This paper	N/A
pMM24-FW, AACAATTTCACAGGGCCCCTCGAGA TTATGTTTGCACAGCAGCCT	This paper	N/A
pMM24-RV, TACGCTTCTTCTTTGGCATGTCATCT GAATAAAGATTATGTATTG	This paper	N/A
pMM24-FW-UTR, AACAATTTCACAGGGCCCCT CGAGATTATGTTTGCACAGCAGCCT	This paper	N/A
pMM24-RV-UTR, TACGCTTCTTCTTTGGCATGTC ATCTGAATAAAGATTATGTATTG	This paper	N/A
pMM27-FW, GGATAACAATTTCACAGGGCCCC TCGAGGTAGATCTACGGAAGTGAACAT	This paper	N/A
pMM27-RV, AAGTGAAGAAGTGGAAATCATTTT TGTTTTTTAAAAATCAAGTGAATGAC	This paper	N/A
pMM33-A-FW, ATTCGATATTTTAAATAA TCTTCTGACTT	This paper	N/A
pMM33-A-RV, TCCCATTCCGTATCCTCCC	This paper	N/A
pMM34-B-FW, ATGTGGGGAAGCCCATAC	This paper	N/A
pMM34-B-RV, GTATCCCCACTGGGCG	This paper	N/A
GFP-NLS-FW, ATGCCAAAGAAGAAGCGTAAGGT GTCAGGTGGATCTGGAGG	This paper	N/A

(*Continued on next page*)

Continued

REAGENT or RESOURCE	SOURCE	IDENTIFIER
GFP-RV, TCATTTGTAAAGTTCATCCATTCC	This paper	N/A
Scarlet-NLS-wrmScarlet-FW, ATGCCAAAGAAGAA GCGTAAGGTGGTCAGCAAGGGAGAGG	This paper	N/A
wrmScarlet-RV, GATGACAGCGGCCGATGCGGA GCTCCTTGTAGAGCTCGTCCATTC	This paper	N/A
BB-FW, CCAAAGAAGAAGCGTAAGGTG	This paper	N/A
BB-RV, CTCGAGGAATTCCTGCAGG	This paper	N/A
Nlp-27 JEP965, CGGTGGAATGCCATATGGTG	Zugasti et al.[55]	N/A
Nlp-27 JEP966, ATCGAATTTACTTTCCCCATCC	Zugasti et al.[55]	N/A
Nlp-28 JEP967, TATGGAAGAGGTTATGGTGG	Zugasti et al.[55]	N/A
Nlp-28 JEP968, GCTAATTTGTCTACTTTCCCC	Zugasti et al.[55]	N/A
Nlp-29 JEP952, TATGGAAGAGGATATGGAGGATATG	Zugasti et al.[55]	N/A
Nlp-29 JEP848, TCCATGTATTTACTTTCCCCATCC	Zugasti et al.[55]	N/A
Nlp-31 JEP950, GGTGGATATGGAAGAGGTTATGGAG	Zugasti et al.[55]	N/A
Nlp-31 JEP951, GTCTATGCTTTTACTTTCCCC	Zugasti et al.[55]	N/A
Nlp-34 JEP969, ATATGGATACCGCCCGTACG	Zugasti et al.[55]	N/A
Nlp-34 JEP970, CTATTTTCCCCATCCGTATCC	Zugasti et al.[55]	N/A
HK_act1_FW, ACGACGAGTCCGGCCCATCC	Zhang et al.[56]	N/A
HK_act1_RV, GAAAGCTGGTGGTGACGATGGTT	Zhang et al.[56]	N/A
tracrRNA, AACAGCAUAGCAAGUUAAAAUAAGG CUAGUCCGUUAUCAACUUGAAAAAGUG GCACCGAGUCGGUGCUUUU	This paper	N/A
ssODN *nlp-27*, CAGGTAGAATACAGAAAACTTA TTTACAAGTTTTTCAAAGAAATATCATTTTTGT TATCTTACTCGCAAACTTTGAAACATGT ATCTAAAGAAACGAAGA	This paper	N/A
crRNA *nlp-27*, ATTCCACCGTATCCACCATA	This paper	N/A
Recombinant DNA		
pCFJ151, pCFJ151 *eft-3(p)::EmGFP::unc-54* 3′ UTR	Gift from Dillin Lab, UC Berkeley and gift from Abby Dernburg	(Addgene plasmid # 71719 ; http://n2t.net/addgene: 71719 ; RRID: Addgene_71719)[57]
myo-2::tdTomato, *myo-2(p)::tdTomato*	Gift from Dillin Lab, UC Berkeley	N/A
myo-2::GFP, *myo-2(p)::GFP*	Gift from Dillin Lab, UC Berkeley	N/A
pVB01, pCFJ151 *nlp-27(p)::nlp-27::nlp-27* 3′ UTR	This paper	N/A
pVB02, pCFJ151 *nlp-29(p)::nlp-29::nlp-29* 3′ UTR	This paper	N/A
pMM15, pCFJ151 *nlp-27(p)::NLS-Scarlet::unc-54* 3′ UTR	This paper	N/A
pMM18, pCFJ151 *col-12(p)::nlp-27::col-12* 3′ UTR	This paper	N/A
pMM19, pCFJ151 *sra-6(p)::nlp-27::sra-6* 3′ UTR	This paper	N/A
pMM24, pCFJ151 *dcar-1(p)::NLS-GFP::dcar-1* 3′ UTR	This paper	N/A
pMM26, pCFJ151 *nlp-27(p)::nlp-27-Scarlet::nlp-27* 3′ UTR	This paper	N/A
pMM27, pCFJ151 *nlp-29(p)::NLS- GFP::unc-54* 3′ UTR	This paper	N/A
pMM33, pCFJ151 *nlp-27(p)::nlp-27A::nlp-27* 3′ UTR	This paper	N/A
pMM34, pCFJ151 *nlp-27(p)::nlp-27B::nlp-27* 3′ UTR	This paper	N/A
pL4440nlp-27, L4440 *T7(p)::nlp-27::T7(p)*	Source Bioscience	N/A
Software and algorithms		
ImageJ	Schindelin et al.[58]	https://imagej.nih.gov/ij/
GraphPad Prism 10.0.3	GraphPad	https://www.graphpad.com/scientific-software/prism/

RESOURCE AVAILABILITY

Lead contact

Further information and requests for resources and reagents should be directed to and will be fulfilled by the lead contact, Reinhard Fischer (Reinhard.fischer@kit.edu).

Materials availability

All strains and plasmids will be available upon request to the lead contact.

Data and code availability

- All data reported in this paper will be shared by the lead contact upon request.
- This paper does not report original code.
- Any additional information required to reanalyze the data reported in this paper is available from the lead contact upon request.

EXPERIMENTAL MODEL AND STUDY PARTICIPANT DETAILS

C. elegans strains were cultured and maintained using standard conditions as described.[53] Bristol N2 was used as the wild type control unless otherwise indicated. All strains were obtained from Caenorhabditis Genetics Centre (CGC) unless stated otherwise. Strains used in this study are described in the key resources table. All the constructed strains express the constructs as an extrachromosomal array. We used empty vector control in the experiments assessing the transgenic lines expressed as extrachromosomal arrays.

The following bacterial strains were used: *Escherichia coli* strain OP50.[53] Bacterial cultures were grown overnight in 4 mL of Luria-Bertani (LB) broth at 37°C. We used standard concentrations of OP50 (Wormbook). Same OP50 concentration was used for both control and the test.

A. flagrans wild type was obtained from the CBS-KNAW Fungal Biodiversity Centre, Utrecht, The Netherlands.

Plasmids are listed in the key resources table, and the oligonucleotides used for constructing them are listed in the key resources table. Oligonucleotides used for qRT-PCR and for the CRISPR/Cas9 deletion are listed in the key resources table.

METHOD DETAILS

qRT-PCR

For RNA extraction synchronized worms already infected were collected with DEPC water and frozen. RNA was extracted in TRIzol with isopropanol and later the DNA was digested using Turbo DNA-free Kit Invitrogen. The total RNA was diluted to a concentration of 50ng/μL. The Luna Universal One-Step RT-qPCR KIT (NEB) was used according to the manufacturer's instructions. The brand and model of the machine used to conduct the qRT-PCR is Bio-Rad iCycler iQ™ Real-Time PCR Detection System. The relative fold changes of the transcripts were calculated using the comparative Ct ($2^{-\Delta\Delta Ct}$) method. For relative expression $2^{-\Delta Ct}$ was presented for each condition. *act-1* was used to normalize the Ct value of the genes. Unpaired Student's t-test or one-way ANOVA was calculated for all experiments. ns P>0.05, *P<0.05, **P<0.01, ***P<0.001. Error bars represent standard deviation. At least three biological replicates and two technical replicates were performed for each qRT-PCR experiment. Primers are listed in the key resources table. The primers used for qRT-PCR span the exons regions. We tested the primers against the *A. flagrans* database, and the primers are specific to *C. elegans*. The *nlp-27* primer pair is specific only to the respective mRNA region when considering product length shorter than 300bp and larger than 70bp. The other pairs of primers have a lower specificity. *nlp-34* primer pair also targets R13D11.10, *nlp-31* primer pair also targets *nlp-29* and *nlp-29* primer pair also targets *nlp-31* and *nlp-30* while *nlp-28* also targets *lonp-1*.

CRISPR/Cas9 knock-out

For CRISPR/Cas9 the mix was prepared as follows: 1.5 μL 100 μM trRNA and 1.1 μL 200μM crRNA incubated at 95°C for 5 min and 25°C for 5 min then added onto 1 μl Cas9 2.5 ng/μl and incubated at 25°C for 5 min. 12.5 ng/μl *myo-2::mCherry* was added as a transformation marker and all was resuspended in IDT buffer to a total volume of 10 μl. All reagents used in the CRISPR/Cas9 mix were acquired from Integrated DNA Technologies (IDT). The oligonucleotides used are listed in the key resources table.

Cultivation of *A. flagrans*

A. flagrans was grown on solid PDM with 1.5 % agar at 28°C for 7 days. The spore solution was prepared by flushing the plate with water and scratching the mycelium off the plate and filtering the solution through miracloth to collect the spores in the water without mycelium.

C. elegans infection assay

The infection assay with *A. flagrans* was used to determine the gene expression of the nematode as a response to fungal infection. The worms to be observed were age-synchronized and used in the L4-young adult stage. The day before, LNA petri dishes were inoculated with *A. flagrans* spores and induced using wild type worms. On the day of the infection assay, the wild type nematodes used to induce the traps were rinsed and the synchronized nematodes were distributed onto the plates. After 4 hours or 24h incubation the plate was gently washed to

remove the untrapped nematodes which were discarded. Afterwards, the plate was washed and scraped with a spatula to collect all the trapped nematodes. The collected nematodes were flash frozen in liquid nitrogen to later be used in RNA extraction.

C. elegans virulence assay

The virulence assay was used to determine the time it takes for the worm to become paralyzed during *A. flagrans* infection. The worms to be observed were age-synchronized and used in the L4 larval stage. The day before, LNA pads were inoculated with *A. flagrans* spores and induced using wild type worms. On the day of the virulence assay, the wild type worms used to induce the traps were rinsed and the inoculated agar was transferred in a microscopy chamber using a spatula. The positions of the traps were first recorded and 10 µl of the synchronized nematodes were distributed in each chamber with inoculated agar pads and observed for 12 hours. Worms were assayed for movement every 5 to 15 minutes depending on the numbers of worms in the sample. All experiments were performed in at least biological duplicates and the experimenters were blinded to the experimental group. The moment of trapping was considered the start of the time count. The last image capture which showed significant movement was considered to be the end of the time count. The amount of time is considered to be the "time to paralysis". A significant movement is considered a movement larger than the width of the worm. On average, 500 hundred worms were used in each replicate of the paralysis assay. Of these only a percentage of them were trapped. On each paralysis graph we display the mean and standard deviation. We used unpaired Student's t-test to quantify the statistical difference.

C. elegans lifespan

The synchronized L4 larvae were transferred to NGM + *E. coli* OP50. Day 0 was considered when nematodes were at the L4 larval stage. A nematode was counted as alive if there was movement. The nematodes that showed no movement were gently touched with a platinum wire and for a few seconds it was observed if there was a movement reaction. If there was no active movement even after repeated touching, they were documented as dead and removed from the plate. If the nematodes showed vulval protrusion, they were removed from the experiment and censored. The data obtained from the lifespan assay was then used to plot a survival curve. The experiments were repeated in biological triplicates at least at two different time points with a minimum of 50 worms per replicate. All experiments were conducted at 20°C and no FUdR was used. The Kaplan-Meier method was used to calculate the survival fractions, and statistical significance between survival curves was determined using the log-rank test. Experimenters were not blinded to the experimental group. However, since there is no significant difference in the observed phenotypes, we did not repeat this experiment in a blind manner. The worms were checked on the following days for movement: 2, 4, 6, 8, 10, 12, 14, 16, 18, 20, 21, 22.

C. elegans PVD dendrite degeneration quantification

PVD dendrite degeneration was characterized as bead or bubble-like structures along the neuron processes. The strain used to observe the neurodegeneration phenotype expresses GFP under *F49H12.4* promoter (key resources table). These structures were quantified using the 40x magnification. Nematodes were considered to have neurodegeneration in the dendrites if a total of ten or more of these structures were observed in more than five menorahs and was reported as a percentage. All experiments were performed in biological triplicates. 30 to 50 worms were used in the experimental assays per replicate and at least three replicates. On each neurodegeneration graph we display a bar with the percentage of nematodes with dendrite degeneration and standard deviation. The brand of the microscope used in the neurodegeneration experiments is Axio Imager Z1 Zeiss. One-way ANOVA statistical test was used to compare the neurodegeneration observed.

C. elegans sterile wounding

The young adults were place on an injection pad and wounded using a sterile microinjection needle after which they were washed with M9 and placed on nematode growth medium (NGM). After 30 minutes the worms were placed onto LNA containing 15 mM NaN_3 and used for microscopy.

C. elegans amphid neurons staining with DiO

The nematodes were stained with DiO as previously described by.[26] Briefly, young adults were washed in M9 buffer and incubated for 2 hr at room temperature with 300 ul of fresh M9 containing DiO 1:150. After incubation the nematodes were washed with M9 and placed on NGM with OP50 for at least 30 minutes before they were used for microscopy. DiO Cell-Labeling Solution stain was acquired from Thermo Fisher Scientific.

RNAi treatment

L1 larvae were grown on *E. coli* strain HT115 (DE3) containing either the empty vector L4440 plasmid or the RNAi treatment plasmid containing *nlp-27* ORF on NGM with IPTG. The plasmids were acquired from Source BioScience. After reaching the young-adult stage the nematodes were used in the virulence assay as described above to assess the time to paralysis.

QUANTIFICATION AND STATISTICAL ANALYSIS

Statistical analyses were conducted using GraphPad Prism version 10.0.3 for Windows, GraphPad Software, www.graphpad.com. For the comparison of mean values between two independent groups, the Student's t-test was applied. One-way ANOVA was used to assess the mean between three or more independent groups. Lifespan assays were analyzed using the Kaplan-Meier survival analysis method, with differences in survival distributions evaluated using the log-rank (Mantel-Cox) test. All experiments were conducted at least in triplicate, with an average of 50 worms per replicate unless stated otherwise. Results were considered statistically significant at a p-value of <0.05.